In vitro reduction of bovine oocyte ATP production with oligomycin affects embryo epigenome

In vitro reduction of bovine oocyte ATP production with oligomycin affects embryo epigenome

Ben Meulders[1], Jo L.M.R. Leroy[1], Inne Xhonneux[1], Peter E.J. Bols[1], Waleed F.A. Marei[1,2]

[1]*University of Antwerp,* Department *of Veterinary Sciences, Laboratory of Veterinary Physiology and Biochemistry, Gamete Research Centre, Wilrijk, Belgium.*

[2]*Cairo University, Department of Theriogenology, Faculty of Veterinary Medicine, Giza, Egypt.*

Authors:

Ben Meulders: ben.meulders@uantwerpen.be; Universiteitsplein 1, 2610 Wilrijk, Belgium

Jo L.M.R. Leroy: jo.leroy@uantwerpen.be; Universiteitsplein 1, 2610 Wilrijk, Belgium

Inne Xhonneux: inne.xhonneux@uantwerpen.be; Universiteitsplein 1, 2610 Wilrijk, Belgium

Peter E.J. Bols: peter.bols@uantwerpen.be; Universiteitsplein 1, 2610 Wilrijk, Belgium

Waleed F.A. Marei: waleed.marei@uantwerpen.be; Universiteitsplein 1, 2610 Wilrijk, Belgium

Short title

Embryo epigenome depends on oocyte ATP

Keywords

Oocyte, mitochondria, ATP, embryo, epigenetics

Word count

5256

Abstract

This study investigated if oocyte and early embryo epigenetic programming are dependent on oocyte mitochondrial ATP production. A bovine *in vitro* experiment was performed in which oocyte mitochondrial ATP production was reduced using 5nmol/l oligomycin A (OM; ATP synthase inhibitor) during *in vitro* maturation (IVM) compared to control (CONT). OM-exposure significantly reduced mitochondrial ATP production rate in MII oocytes (34.6% reduction, P=0.018) and significantly decreased embryo cleavage rate at 48h post-insemination (7.6% reduction, P=0.031). Compared to CONT, global DNA methylation (5mC) levels were decreased in OM-exposed MII oocytes (9.8% reduction, P=0.019) while global histone methylation (H3K9me2) was increased (9.4% increase, P=0.024). In zygotes, OM-exposure during IVM increased 5mC (22.3% increase, P<0.001) and histone acetylation (H3K9ac, 17.3% increase, P=0.023) levels, while H3K9me2 levels were not affected. In morulae, 5mC levels were increased (10.3% increase, P=0.041) after OM-exposure compared to CONT, while there was no significant difference in H3K9ac and H3K9me2 levels. These epigenetic alterations were not associated with any persistent effects on embryo mitochondrial ATP production rate or mitochondrial membrane potential (assessed at the 4-cell stage). Also, epigenetic regulatory genes were not differentially expressed in OM-exposed zygotes or morulae. Finally, apoptotic cell index in blastocysts was increased after OM-exposure during oocyte maturation (41.1% increase, P<0.001). We conclude that oocyte and early embryo epigenetic programming are dependent on mitochondrial ATP production during IVM.

In brief

Epigenetic programming is a crucial process during early embryo development that can have a significant impact on the results of assisted reproductive technology (ART) and offspring health. Here we show evidence using a bovine *in vitro* experiment that embryo epigenetic programing is dependent on oocyte mitochondrial bioenergetic activity during maturation.

Introduction

Mitochondrial (MT) bioenergetic activity in oocytes and early embryos is crucial for the production of adenosine triphosphate (ATP) (Grindler and Moley, 2013). The oocyte and early embryo require adequate ATP levels to support the molecular changes and cytoskeletal dynamics during nuclear and cytoplasmic maturation (Chappel, 2013, Adhikari et al., 2022a). Reduced oocyte ATP levels are linked with lower fertilization rates and subsequent embryo development (Stojkovic et al., 2001). On the other hand, excessively high ATP levels during oocyte maturation also compromise developmental capacity (Nagano et al., 2006a). During final maturation, oocytes rely

on oxidative phosphorylation (OXPHOS) for ATP production (Sturmey et al., 2009, Paczkowski et al., 2013) and are thus dependent on MT bioenergetic activity (Nagano et al., 2006b, Duran et al., 2011). In contrast, glucose metabolism gradually shifts to aerobic glycolysis (Warburg effect) in the cleavage stages to support cell proliferation (Krisher and Prather, 2012).

MT dysfunction in oocytes is a key causative link to subfertility in maternal health conditions like obesity (Igosheva et al., 2010, Grindler and Moley, 2013) and type 2 diabetes (Wang et al., 2009). Reduced oocyte quality linked to ageing (van der Reest et al., 2021), polycystic ovarian syndrome (PCOS) (Chappell et al., 2021) and heat stress (Gendelman and Roth, 2012) has also been associated with MT dysfunction. Systemic changes such as dyslipidemia and increased inflammatory cytokines are reflected in the ovarian follicular fluid (FF), the microenvironment in which oocyte maturation takes place (Valckx et al., 2012, Piersanti et al., 2019). This results in nutritive overload and oxidative stress, leading to oocyte MT dysfunction associated with reduced ATP production in all these conditions (Igosheva et al., 2010, Marei et al., 2020).

In somatic cells, the link between MT activity and epigenetic programming is generally accepted and well described. Mitochondria produce substrates and co-factors that are required for epigenetic regulation, like ATP, S-adenosylmethionine (SAM), and acetyl-CoA (Castegna et al., 2015, Matilainen et al., 2017). ATP is important for several processes related to epigenetic programming. For example, SAM and acetyl-CoA synthesis are both dependent on ATP availability (Wellen et al., 2009, Teperino et al., 2010). ATP also enhances the enzymatic activity of the ten-eleven translocation (*TET*) enzyme, which catalyzes DNA demethylation (Yin and Xu, 2016). In contrast with somatic cells, the link between MT function and epigenetic regulation is underexplored in oocytes and early embryos. The epigenetic patterns are very particular in oocytes and embryos as they undergo highly dynamic and extensive stage-specific epigenetic reprogramming. While DNA methylation levels significantly increase during oocyte maturation, extensive global DNA demethylation occurs shortly after fertilization followed by *de novo* methylation during early embryo development, together with stage-specific histone modifications (Okano et al., 1999, Morgan et al., 2005, Ge and Sun, 2019).

The above mentioned epigenetic and metabolic dynamics make it difficult to define the potential direct impact of suboptimal mitochondrial ATP production during oocyte maturation on subsequent embryo epigenetic programming. The oocyte epigenome appears to be sensitive to changes in the microenvironment (Schierding et al., 2017). This is illustrated by different studies that showed that e.g. diet-induced obesity in mice significantly altered global DNA methylation and histone modifications in oocytes (Ge et al., 2014, Hou et al., 2016). However, since the epigenome is globally demethylated and reprogrammed afterwards, the importance of the oocyte MT

bioenergetic functions and epigenetic patterns for setting up epigenetic programming in the next stages of embryo development is not known.

Currently, *in vitro* maturation (IVM) is introduced in human *in vitro* fertilization (IVF) practice (Chang et al., 2014) and various promising *in vitro* MT therapies exist to improve MT functions either in oocytes or in embryos. Nevertheless, the importance of the timing of these treatments to assure optimal epigenetic programming is less defined. For example, a few studies suggest the use of mitochondrial targeted antioxidants (e.g. MitoQ) either during IVM or *in vitro* culture (IVC) to support mitochondrial activity and minimize cellular stress induced by lipotoxicity or ageing, which has been linked with increased embryo developmental competence and number of transferable embryos (Marei et al., 2019, Al-Zubaidi et al., 2021). It is not known if the efficiency of MT bioenergetic functions during oocyte maturation would affect subsequent embryo epigenetic programming.

In the present study, we hypothesized that the epigenetic changes which take place not only during oocyte maturation, but also during early embryo development are both dependent on oocyte MT bioenergetic activity (ATP production). To test this hypothesis, we exposed bovine cumulus-oocyte complexes (COCs) to oligomycin A (OM, an inhibitor of the MT electron transport chain (ETC) ATP synthase (complex V)) during IVM (for 24h). We used a pre-optimized concentration of 5nmol/l OM that results in a partial and temporary reduction in oocyte MT ATP production, which is then subsequently restored in embryos. We tested the impact of the reduction in oocyte MT ATP production on global DNA methylation (5mC), histone acetylation (H3K9ac) and histone methylation (H3K9me2) levels in oocytes and during early embryo development. Expression of epigenetic regulatory genes in early embryos was also measured to examine the mechanisms involved.

Materials and methods

Material

All chemicals were purchased from Merck Life Science (Hoeilaart, Belgium) unless otherwise stated.

Experimental design

During IVM, bovine COCs (14 replicates, ≈140 COCs/treatment/replicate) were evenly distributed over 2 treatment groups: control (CONT) and 5nmol/l oligomycin A (OM), a complex V inhibitor (Symersky et al., 2012) and a widely used modulator of ATP levels in somatic cells (Leist et al., 1997). OM has also been previously used in experiments determining ATP levels in oocytes (Blerkom et al., 2003) and oxygen consumption rate (OCR) in embryos (Li et al., 2021). A concentration range of 5nmol/l to 2µmol/l OM for 30min or 24h IVM was tested in preliminary experiments. Exposure to 5nmol/l OM for 24h resulted in a decrease of MII oocyte ATP production

rate and also reduced cleavage and blastocyst rates (see supplementary annex). IVF and IVC both occurred under standard conditions.

Firstly we examined if OM decreases ATP production in MII oocytes (5 replicates, 1-2 measurements/group/replicate, pools of 13 oocytes). Developmental competence was assessed with maturation rate (3 replicates), embryo cleavage rates and day 7 & day 8 blastocyst rates (4 replicates). Also, blastocyst quality was assessed with caspase-3/CDX-2/Hoechst immunostaining (4 replicates). We then assessed the effect on 5mC levels in MII oocytes, (3 replicates, 34/treatment), zygotes (3 replicates, 26/treatment) and morulae (3 replicates, 23-30/treatment). Then, the same was done for H3K9ac and H3K9me2 levels in MII oocytes (3 replicates, 33-35/treatment), zygotes (3 replicates, 25-26/treatment) and morulae (5 replicates, 33-36 embryos/treatment). Although OM was not added to the IVF and IVC media, we also wanted to rule out direct effects of a potential persistent OM-induced MT dysfunction during embryo development. Therefore we tested the ATP production rate (3 replicates, pools of 20 embryos) and MT membrane potential (MMP) (3 replicates, 32/treatment) in the embryos (assessed at the 4-cell stage). Finally, to determine if OM-induced alterations in epigenetic patterns are associated with transcriptomic alterations, we examined the gene expression of marker genes involved in epigenetic regulation in zygotes (6 replicates, 20 embryos/pool) and morulae (3-6 replicates, 20 embryos/pool) (Fig. 1).

Collection and selection of bovine COCs

Bovine ovaries were collected from a local abattoir in warm saline solution (NaCl 0.9% (w/v)) and transferred to our laboratory within 3h. Next, they were washed twice in NaCl 0.9% (w/v) (37°C) supplemented with 0.0025% kanamycin (w/v). Antral follicles with 2-6mm diameter were aspirated using a 10ml syringe with 18G needle. After aspiration, the FF was collected in 15ml tubes and centrifuged for 1 min at 13g. The precipitate was then transferred to a 90mm petri dish containing Hepes-buffered Tyrode's albumin lactate pyruvate media (Wash-TALP). Quality grade I COCs (unexpanded with dark homogeneous ooplasm surrounded by five or more cumulus cell layers) were selected under an Olympus SZX7 stereomicroscope (Marei et al., 2012).

In vitro maturation (IVM)

Maturation medium consisted of TCM-199 medium with cysteamine (0.1µmol/l), sodium pyruvate (0.2mmol/l), L-glutamine (0.4mmol/l), gentamicin (0.1mmol/l) and murine epidermal growth factor (3.3nmol/l). COCs were washed in droplets of Wash-TALP and transferred to equilibrated four-well plates in groups of 40-60 COCs (10µl maturation medium/COC). In the OM group, 0.5% (v/v) of a 1µmol/l OM-stock solution (Agilent Technologies, Machelen, Belgium; prepared in Medium-199) was added to the maturation medium to obtain a final concentration

of 5nmol/l OM. In the CONT group, 0.5% Medium-199 (v/v) was added for comparison with the OM group. Plates were incubated for 24h in a humidified atmosphere with 5% CO_2 at 38.5°C. According to the experimental design, COCs were collected at the end of IVM for denudation and assessment of ATP production rate in the oocytes, fixation for assessment of 5mC and H3K9ac/H3K9me2 or IVF (see further). In oocytes that were used for 5mC immunostaining, maturation rate was also assessed (3 replicates).

In vitro fertilization (IVF)

COCs were washed and transferred to fertilization medium (Fert-TALP medium containing 0.72 IU/ml heparin) with 10^6 spermatozoa/ml in four-well plates (40-110 COCs/well) after 24h IVM. Frozen bull semen from the same ejaculate with proven *in vitro* fertility was used for IVF. Using a Percoll gradient (90-45%), motile spermatozoa were separated by centrifugation for 10min at 971g and 10min at 155g. COCs were co-incubated with spermatozoa for 20h in a humified atmosphere with 5% CO_2 at 38.5°C.

In vitro culture (IVC)

Presumptive zygotes were vortexed for 3min in Wash-TALP for denudation and then washed in droplets of 100µl Wash-TALP at 20h after IVF. They were then transferred to a 96-well plate in groups of 25 ± 3 in 75µl of synthetic oviductal fluid containing 2% BSA (w/v) (without oil) (Desmet et al., 2018). Embryos were incubated in 90% N_2, 5% CO_2, 5% O_2 at 38.5°C until day 4.7 post-insemination (p.i.) for morula collection, or until blastocyst stage on day 8 p.i..

At 48h p.i., embryos were assessed under the inverted light microscope (Olympus CKX41) and classified as not-cleaved, 2-cell, 3-cell, 4+ cells or fragmented (cells are not uniform in colour and density and/or asymmetric). On day 7 and day 8 p.i., blastocyst rates were recorded and classified as young (blastocoel is smaller than inner cell mass (ICM)), normal (blastocoel is larger than ICM), expanded (increased size, thinning of zona pellucida and/or blastocoel/ICM ratio exceeds 70/30) or hatched (zona pellucida is not intact) blastocysts.

According to the experimental design, zygotes (24h p.i.), 4-cell embryos (48h p.i.) and/or morulae (day 4.7 p.i.) were collected. Collected zygotes and morulae were fixed for assessment of 5mC and H3K9ac/H3K9me2 levels, while other zygotes and morulae were snap-frozen for assessment of mRNA transcript abundance. 4-cell embryos were collected for assessment of MMP or MT ATP production rate. In these replicates, IVC was terminated at the 4-cell or morula stage.

ATP production rate

Preparation and analysis were performed as in Muller et al. (2019). COCs were collected after 24h IVM in 0.03% hyaluronidase (w/v) in Wash-TALP for denudation. 4-cell embryos were collected in Wash-TALP at 48h p.i.. Then, oocytes or embryos were washed in Seahorse analysis medium (Seahorse XF DMEM assay medium with 10mmol/l Seahorse XF glucose solution, 1mmol/l Seahorse XF pyruvate solution and 2mmol/l Seahorse XF glutamine solution) and transferred to a Seahorse XFp Cell Culture Miniplate filled with Seahorse analysis medium in pools of 13 oocytes or 20 4-cell embryos. Then, the ATP Rate Assay was performed following the manufacturer instructions. During the assay, both oxygen consumption rate (OCR) and extracellular acidification rate (ECAR) were measured in real-time within the wells containing the oocytes or 4-cell embryos. After the 3 first measurements, 2.5µmol/l oligomycin A (which is different from the 5nmol/l oligomycin A added during IVM in the OM group) was injected in the wells to inhibit complex V of the ETC. After 3 more measurements, 0.5µmol/l of a Rotenone/Antimycin A mixture was injected in the wells to inhibit complex I and III of the ETC, followed by 3 final measurements. MT ATP production rate is the OCR that is coupled to ATP production during OXPHOS and can be calculated by the change in OCR after injecting a high concentration of OM (2.5µmol/l) during the assay: OCR_{ATP} (pmol O_2/min) = OCR (pmol O_2/min) – OCR_{OM} (pmol 0_2/min).

Total cell number and apoptotic cell index

Blastocysts were collected at day 8 p.i., fixed in 4% paraformaldehyde (PFA) (w/v) for 15min and stored in 0.1% (w/v) polyvinylpyrrolidone (PVP) in Phosphate Buffered Saline (PBS) (PBS-PVP). All blastocysts were immunostained and imaged as previously described by Wydooghe et al. (2011) using a mixture containing 1:1 mouse-anti-CDX2 (Biogenex, CA, USA) and rabbit-anti-cleaved Caspase-3 (1:250 dilution, Cell Signaling, Leiden, The Netherlands) as primary antibodies and a mixture containing FITC-labelled goat anti-rabbit and Texas-red labelled goat anti-mouse secondary antibodies (1:200 each, Thermo Fisher Scientific). Negative staining controls remained in the blocking solution. Counter-staining of the nuclei was performed with Hoechst (5µg/ml) in PBS-PVP for 10min. An image of each blastocyst was acquired using a fluorescence microscope (Olympus IX71, X-cite series 120 Q) at 20X at excitation/emission of 360-370/420-460 nm (Hoechst to determine total cell numbers), 570/595 nm (Texas-red to count trophectoderm (TE) cells), and 460-490/520-540 nm (FITC-positive apoptotic cells). Using Cell Sens-Standard software, total cells, TE cells, ICM cells and apoptotic cells were counted. This data is presented regardless the blastocyst stage or focusing only on early blastocysts (young and normal), or only advanced blastocysts (expanded and hatched). See supplementary figure S2 for representative images.

Global DNA methylation and histone methylation/acetylation

Oocytes, zygotes and morulae were fixed in 4% PFA (w/v) for 15min and stored in PBS-PVP. All oocytes and embryos were immunostained and imaged as previously described (Dobbs et al., 2013, Wu et al., 2020) using primary antibodies (5mC: rabbit 5mC, Cell Signaling, 1:1600 dilution; H3K9ac: mouse H3K9ac, Abcam, Cambridge, United Kingdom – 1:500 dilution; H3K9me2: rabbit H3K9me2 antibody, Cell Signalling, 1:250) and secondary antibodies (5mC/H3K9me2: goat anti-rabbit FITC secondary antibody, Thermo, 1:200 dilution; H3K9ac: goat anti-mouse Texas-Red antibody, Thermo, 1:200 dilution). Equivalent concentrations of normal rabbit or mouse IgG were used for the negative controls instead of the primary antibodies. Then, oocytes and embryos were mounted in DABCO droplets and examined under a SP8 confocal microscope (Leica, Diegem, Belgium) equipped with white laser source (WLL) at excitation/emission 488/525 nm (to visualize FITC-labelled 5mC or H3K9me2) and 530/620 nm (for Texas-red labelled H3K9ac). Scanned depth was 14µm with 1µm interval. Using ImageJ software, the gray scale intensity of every channel in each nucleus at each z-stack was quantified and averaged to generate an average mean gray intensity of 5mC, H3K9ac and H3K9me2 for each oocyte or embryo. See supplementary figures S3, S4 and S5 for representative images.

Mitochondrial membrane potential (MMP)

In 4-cell stage embryos, MMP was assessed at 48h p.i. by a JC-1 (5,5',6,6'-tetrachloro-1,1',3,3'-tetraethyl-benzimidazolyl-carbocyanine iodide, Thermo) fluorescence staining as described by Marei et al. (2019). 4-cell stage embryos were incubated in Wash-TALP with JC-1 (5µg/mL) (from 1000× stock solutions in dimethyl sulfoxide) for 30 min at 5% CO_2, 5% O_2 at 38.5°C. Next, they were washed and transferred to Wash-TALP droplets in 35 mm glass-bottom dishes covered with mineral oil. Embryos were examined under a SP8 confocal microscope (Leica) in a controlled environment (37°C) and equipped with WLL at excitation/emission 488/525 nm (to visualize green JC-1 monomers indicating MT with low MMP) and 561/590 nm (for the yellow JC1-aggregates which are formed when MMP is high). Using ImageJ, the gray scale intensity of the blastomeres in each channel in the mid-plane and subcortical area of the embryo was quantified. MMP was calculated as a ratio of the gray scale intensity at 590:525 nm. See supplementary figure S6 for representative images.

Gene expression

Pools of 20 zygotes (24h p.i.) or morulae (day 4.7 p.i.) were washed in PBS-PVP droplets, transferred in minimal volume to a 1.5ml vial, and immediately snap-frozen in liquid nitrogen and stored at −80°C. PicoPure RNA Isolation Kit (Thermo) was used for RNA extraction. RNA samples were treated with DNase (Qiagen, Hilden,

Germany), and cDNA was synthesized using Sensiscript RT kit (Qiagen). Quantification of mRNA transcripts was performed by quantitative polymerase chain reaction (real-time PCR, qPCR) using 8µl SYBR Green, 0.2µl forward primer, 0.2 reverse primer, 4.6µl H_2O and 3µl cDNA per well. No reverse transcription (NRT) and no template control (NTC) were included. Quantification results were normalized using the geometric mean of the housekeeping genes 18S ribosomal RNA (*18S*) and tyrosine 3-monooxygenase/tryptophan 5-monooxygenase activation protein zeta (*YWHAZ*). Then, the relative expression of each gene was calculated using the 2^-ΔΔCT method (Pfaffl, 2001). Target genes were chosen based on their role in epigenetic processes during early embryo development and also considering their stage-specific expression patterns (*Table 1 and Supplementary table S2*).

Statistical analysis

Statistical analyses were performed using IBM Statistics SPSS 28 (for Windows, Chicago, IL, USA). Categorical data were compared with binary logistic regression. Numerical data were tested for normality of distribution (Kolmogorov-Smirnov test) and homogeneity of variance (Levene's test) and the means were compared with a two-sided independent samples t-test. ATP production rate, blastocyst quality, H3K9me2 in zygotes, MMP and mRNA expression were not normally distributed and thus analysed using a Mann-Whitney-U test. Interaction between group and IVP replicate effects was tested. If the interaction term was not significant it was left out from the final model. A p-value of ≤0.05 was considered as significant (indicated with different superscripts "a" and "b").

Results

MT ATP production rate in oocytes following OM exposure

MT ATP production rate was measured in the oocytes treated with or without OM for validation. OM-exposure led to a significant decrease in MT ATP production rate in the oocytes compared with CONT (P=0.018) (*Fig. 2*).

Effect of inhibition of oocyte ATP synthesis on developmental competence

OM-exposure during IVM did not affect oocyte maturation rate compared to CONT (91.7 ± 4.8% vs 91.1 ± 0.6%), but resulted in a significant decrease in embryo cleavage rate at 48h p.i. (P=0.031) and tended to reduce development to the blastocyst stage (P=0.051). Other parameters of developmental competence were not significantly altered (P>0.05) (*Table 2*).

Effect on blastocyst quality

OM-exposure significantly reduced total cell counts in advanced blastocysts only (P=0.018). TE cell count was only reduced significantly compared to CONT when focusing on the advanced blastocysts (P=0.009). ICM cell count and TE/ICM ratio were not affected by OM (P>0.1). OM-exposure significantly increased apoptotic cell index in the advanced blastocysts compared to CONT (P<0.001, *Table 3*).

Effect on global DNA methylation

OM-exposure during IVM significantly decreased 5mC levels in MII oocytes compared to CONT (P=0.019). In contrast, 5mC levels were significantly increased in zygotes (P<0.001) and morulae (P=0.041) derived from OM-treated oocytes compared to CONT (*Fig. 3*).

Effect on histone modifications

H3K9ac levels are erased in MII oocytes (Gu et al., 2010), and was not detectable here in oocytes. OM-exposure significantly increased H3K9ac levels in zygotes compared with CONT (P=0.023), while there was no effect on H3K9ac levels at the morula stage (P>0.1) (*Fig. 4a*). OM-exposure significantly increased H3K9me2 levels in MII oocytes compared to CONT (P=0.024). In contrast, OM did not affect H3K9me2 in zygotes and morulae (P>0.1) (*Fig. 4b*).

Potential persistent effects on mitochondrial bioenergetic activity in embryos

The effect of OM on oocyte MT ATP production was not persistent in subsequently produced embryos, since no significant differences in MMP (Fig. 5a) and MT ATP production rate (Fig. 5b) could be detected between the treatment groups.

Gene expression

The relative mRNA abundance of *DNMT3B, TET2, TET3, EHMT1, EHMT2, HAT1 and HDAC3* at the zygote stage did not differ between the OM and CONT group (P>0.1) (*Fig. 6a*). In morulae, the relative mRNA abundance of *DNMT3A, TET1*, *EHMT1*, *KDM3A*, *HAT1* and *HDAC2* did not differ between the OM and CONT group (P>0.1) (*Fig. 6b*).

Discussion

The aim of this study was to examine if the epigenetic programming during early embryo development is dependent on MT ATP production during the final phase of oocyte maturation. Bovine COCs were exposed to

5nmol/l OM during IVM to reduce oocyte MT ATP production. As expected, this reduces developmental competence, lowers cell numbers and increases apoptotic cell index in day 8 blastocysts. Interestingly, the reduction in ATP production was not only linked with altered 5mC and H3K9me2 levels in the exposed MII oocytes, but also with increased 5mC and H3K9ac in the subsequently produced zygotes and increased 5mC in the morulae, despite the fact that the MT bioenergetic capacity was normalized after the removal of OM from the media during IVF and IVC. These effects could not be explained by differences in the expression of epigenetic regulatory genes in early embryos and are clearly dependent, directly or indirectly, on oocyte ATP levels.

Harvey (2019) hypothesized that MT activity and the availability of MT metabolites in oocytes and embryos may be essential in epigenetic modification, like in somatic cells. Only recently, few studies investigated this important link in the female gamete. For example, deletion of the MT fission factor *DRP1* in murine oocytes resulted in altered 5mC and H3K27me3 levels in oocytes and zygotes (Adhikari et al., 2022b). Obviously, the impact of *DRP1* deletion does not only influence MT functions in oocytes but persists throughout subsequent development. Also, culturing bovine embryos with sodium-iodoacetate or dichloroacetate to disrupt the glycolytic pathway or increase acetyl-CoA production reduced and increased H3K9ac, respectively, in the resulting blastocysts (Ispada et al., 2021). These are direct effects of altered embryo metabolism. As explained before, ATP plays an important role in establishing epigenetic marks in somatic cells (Wellen et al., 2009, Teperino et al., 2010, Yin and Xu, 2016). However, to the best of our knowledge, the effect of altered MT ATP production in oocytes during final stage of maturation on epigenetic programming in oocytes and embryos has not been described.

Global DNA methylation levels increase during oocyte maturation and reach maximal levels at the MII stage (Ge and Sun, 2019). Here, we demonstrated a significant reduction in 5mC levels in MII oocytes after OM-exposure compared to control. S-adenosyl methionine transferase depends on intracellular ATP levels for the conversion of methionine to SAM (Teperino et al., 2010). A reduction in ATP production is therefore expected to decrease SAM levels and thus reduce global DNA methylation in the oocytes. Based on this result, it appears that this mechanism also takes place in oocytes and that oocyte global DNA methylation is dependent on simultaneous MT ATP production during maturation. Given that DNA methylation is associated with silencing of gene transcription (Smiraglia et al., 2008, Wu et al., 2020), reduced MT bioenergetic activity may alter gene expression after embryonic genome activation (EGA) at the 8-cell stage in bovine embryos (Ross and Sampaio, 2018). High levels of DNA methylation during oocyte maturation are important for reprogramming of genomic imprints (O'Doherty et al., 2012). Inappropriately methylated imprinted loci can lead to abnormal expression of maternal and/or paternal copies (O'Doherty et al., 2014), resulting in pathological events such as neonatal diabetes (Temple and Shield,

2002). This may explain the developmental abnormalities associated with oocyte MT dysfunction due to e.g. obesity (Grindler and Moley, 2013), and we suggest here for the first time that these may be initiated during final oocyte maturation by inadequate ATP synthesis.

Furthermore, H3K9ac levels are erased in MII oocytes (Gu et al., 2010, Wu et al., 2020), while H3K9me2 levels are relatively stable during meiosis (Gu et al., 2010, Wu et al., 2020). OM-exposure increased H3K9me2 levels in oocytes. The different effects of OM on 5mC and H3K9me2 levels might be explained by the fact that 5mC levels increase during final oocyte maturation, while H3K9me2 levels are relatively stable. Also, the inhibition of subunit F0 of the F0/F1 ATPase by OM leads to an accumulation of hydrogen ions in the MT inner membrane space, resulting in a reduced activity of complex I and III of the ETC which may indirectly lead to accumulation of MT metabolites such as alpha-ketoglutarate (Lee and O'Brien, 2010). Alpha-ketoglutarate is a substrate for *TET* enzymes (Lu and Thompson, 2012) and the observed reduction in 5mC levels in MII oocytes may thus be caused by an increased DNA demethylation by *TET* enzymes. H3K9me2 levels are important in the formation of inactive or active transcription regions and play a role in chromatin remodeling (Clarke and Vieux, 2015).

After fertilization, genomic DNA undergoes DNA demethylation which continues until the 8-cell stage in bovine embryos (Dobbs et al., 2013). In contrast to the reduced 5mC levels in OM-exposed oocytes, zygotes and morulae derived from OM-treated oocytes had increased 5mC levels. *TET* enzymes are highly active in zygotes (Uh et al., 2020) and their activity is ATP-dependent. (Yin and Xu, 2016). The increase in 5mC levels in zygotes derived from OM-exposed oocytes could therefore be due to a decrease in *TET* enzyme activity, which is different from gene expression that is discussed later, due to the reduced ATP production rate. Importantly, 5mC levels in zygotes were quantified in both pronuclei together, although the male and female pronucleus show different DNA demethylation dynamics. We chose to not quantify them separately as our only aim was to assess global effects on epigenetic patterns. On the other hand, the increased 5mC levels in morulae might also be a result of a compensatory increase in MT bioenergetic functions after fertilization and embryo culture under standard conditions. In a study using human embryos, it was suggested that energetic stress during oocyte development will result in activation of MT biogenesis in embryos as a compensation mechanism (Diez-Juan et al., 2015). To examine this, we measured MMP and MT ATP production in 4-cell embryos produced from OM-treated oocytes, and found that MT bioenergetic activity was restored to the same level as in the embryos derived from control oocytes; i.e. not inhibited anymore but also no compensatory increase. DNA hypermethylation in zygotes may interrupt EGA and thus the initiation of gene expression in further embryo development (Smith et al., 2012). High

DNA methylation levels at the morula stage might hamper this process leading to failing cell differentiation during gastrulation (Hackett and Surani, 2013).

H3K9me2 levels decrease during fertilization whereas these levels increase during preimplantation development (Wu et al., 2020). H3K9me2 levels were not affected by OM in zygotes and morulae. In contrast, H3K9ac levels are expected to increase in zygotes (Wu et al., 2020) and further increase from the morula to the blastocyst stage (Wu et al., 2020). H3K9ac levels were significantly increased in the zygotes following OM-exposure, but were not changed at the morula stage. ATP-citrate lyase is responsible for the conversion of citrate into acetyl-CoA and oxaloacetate (Wellen et al., 2009). A reduction in ATP should thus lead to a depletion in acetyl-CoA and subsequently a decrease in H3K9ac levels in zygotes, which was not the case. The increase in H3K9ac levels might occur due to an increase in NADH/NAD^+ ratio and thus a decrease in NAD^+, which activates histone deacetylases, ultimately leading to increased histone acetylation (Cosentino and Mostoslavsky, 2013). Since reduced ATP levels can both increase and decrease histone acetylation levels, this can explain why no differences were observed at the morula stage. Acetylation of lysine 9 on H3 in the promotor region is associated with gene activation (Kim et al., 2003) while methylation of lysine 9 on H3 is correlated with gene silencing or heterochromatin formation (Mozzetta et al., 2015). Alterations in H3K9ac or H3K9me2 levels might thus affect gene expression patterns later in development at the blastocyst stage.

Finally, we investigated the expression of genes that code for epigenetic regulatory enzymes to see if the reported epigenetic changes might be associated with transcriptomic changes. We expected that the gene expression of some of these markers may change in response, or as a compensation for, the observed alterations in the availability of ATP and potentially other MT intermediate products. Zygotes and morulae are sensitive to their microenvironment since their gene expression can be altered after exposure to heat shock or alterations in O_2 concentration (Balasubramanian et al., 2007, Sakatani et al., 2013). Some studies have reported alterations in expression of these epigenetic regulatory genes. For example, exposure of mice to high-fat diet alters the expression of genes involved in methylation and acetylation processes in ovary, testes and hypothalamus (Funato et al., 2011, Sukur et al., 2023). Also, blastocysts showed altered expression of Sirtuin 1, a gene involved in histone deacetylation, after exposure to increased non-esterified fatty acid concentrations during IVM which is known to induce MT dysfunction in oocytes and embryos (Desmet et al., 2016). However, to the best of our knowledge, this is the first time that the expression of epigenetic regulatory genes has been examined during earlier stages of embryo development. We demonstrated that gene expression levels of all the tested epigenetic regulatory genes in zygotes (*DNMT3B*, *TET2*, *TET3*, *EHMT1*, *EHMT3, HAT1*, and *HDAC3*) and morulae (*DNMT3A*, *TET1*, *EHMT1*,

KDM3A, *HAT1*, and *HDAC2*) were not influenced by the OM-exposure during IVM, compared to the control. This further supports the idea that the reported epigenetic alterations are derived by the alteration in oocyte MT bioenergetic activity. It's important to note that for example protein folding of *HDAC3* is an ATP-dependent process and may thus affect epigenetic programming despite the absence of transcriptomic alterations (Guenther et al., 2002).

Conclusions

In conclusion, we show evidence that reduced oocyte mitochondrial bioenergetic activity during maturation is not only linked with altered 5mC and H3K9me2 levels in the oocyte, but also with altered 5mC and H3K9ac levels in the subsequently formed zygotes and 5mC levels in the morulae. In this in vitro experimental setting, these long-term effects occur despite the recovery of mitochondrial activity and ATP production rate in the affected embryos. Several maternal health conditions like obesity, PCOS and ageing are associated with mitochondrial dysfunction in oocytes. Our results suggest that the reduced oocyte MT ATP production may play a role, at least partly, in the observed epigenetic alterations in the offspring from these patients, regardless of the conditions after fertilization. Our data provide an extra incentive to develop interventions aiming at improving oocyte quality and safeguarding embryo epigenetic programing. These interventions should target the oocyte mitochondria to protect its bioenergetic activity and support optimal ATP production rates already during maturation.

Declaration of interest

The authors declare that there is no conflict of interest that could be perceived as prejudicing the impartiality of the research reported.

Funding

Ben Meulders is supported by a fellowship from the Research Foundation-Flanders (FWO), grant number 11F5821N.

Author contributions

BM was the primary responsible for the design, conducting, data analysis and writing of this experiment. WFAM and JLMRL provided the idea and main research questions and supervised the work. IX assisted with conducting the experiments. PEJB critically revised the manuscript. The first draft of the manuscript was written by BM and all authors commented on previous versions of the manuscript. All authors read and approved the final manuscript.

Acknowledgements

The authors would like to acknowledge ACAM, the microscopy core facility of the University of Antwerp, for the use of their microscopy facilities. The microscope used in this publication, i.e. Leica SP8 (GOH4216N), was funded by a Medium-scale research infrastructure grant of the FWO.

Data repository

In Mendeley Data, all raw datasets are deposited at DOI: 10.17632/gy7t9pf6fs.1, and images of 5mC immunostainings of zygotes are deposited at DOI: 10.17632/5r6bmn5szr.1.

References

Adhikari, D., Lee, I. W., Yuen, W. S. & Carroll, J. 2022a. Oocyte mitochondria-key regulators of oocyte function and potential therapeutic targets for improving fertility. *Biol Reprod,* 106**,** 366-377.

Adhikari, D., Lee, I. W., Al-Zubaidi, U., Liu, J., Zhang, Q. H., Yuen, W. S., He, L., Winstanley, Y., Sesaki, H., Mann, J. R., et al. 2022b. Depletion of oocyte dynamin-related protein 1 shows maternal-effect abnormalities in embryonic development. *Sci Adv,* 8**,** eabl8070.

Al-Zubaidi, U., Adhikari, D., Cinar, O., Zhang, Q. H., Yuen, W. S., Murphy, M. P., Rombauts, L., Robker, R. L. & Carroll, J. 2021. Mitochondria-targeted therapeutics, MitoQ and BGP-15, reverse aging-associated meiotic spindle defects in mouse and human oocytes. *Hum Reprod,* 36**,** 771-784.

Balasubramanian, S., Son, W. J., Kumar, B. M., Okc, S. A., Yoo, J. G., Im, G. S., Choe, S. Y. & Rho, G. J. 2007. Expression pattern of oxygen and stress-responsive gene transcripts at various developmental stages of in vitro and in vivo preimplantation bovine embryos. *Theriogenology,* 68**,** 265-275.

Blerkom, J. V., Davis, P. & Alexander, S. 2003. Inner mitochondrial membrane potential (ΔΨm), cytoplasmic ATP content and free Ca2+ levels in metaphase II mouse oocytes. *Human Reproduction,* 18**,** 2429-2440.

Castegna, A., Iacobazzi, V. & Infantino, V. 2015. The mitochondrial side of epigenetics. *Physiol Genomics,* 47**,** 299-307.

Chang, E. M., Song, H. S., Lee, D. R., Lee, W. S. & Yoon, T. K. 2014. In vitro maturation of human oocytes: Its role in infertility treatment and new possibilities. *Clin Exp Reprod Med,* 41**,** 41-6.

Chappel, S. 2013. The role of mitochondria from mature oocyte to viable blastocyst. *Obstet Gynecol Int,* 2013**,** 183024.

Chappell, N. R., Zhou, B., Hosseinzadeh, P., Schutt, A., Gibbons, W. E. & Blesson, C. S. 2021. Hyperandrogenemia alters mitochondrial structure and function in the oocytes of obese mouse with polycystic ovary syndrome. *F S Sci,* 2**,** 101-112.

Clarke, H. J. & Vieux, K. F. 2015. Epigenetic inheritance through the female germ-line: The known, the unknown, and the possible. *Semin Cell Dev Biol,* 43**,** 106-116.

Cosentino, C. & Mostoslavsky, R. 2013. Metabolism, longevity and epigenetics. *Cellular and molecular life sciences : CMLS,* 70**,** 1525-1541.

Desmet, K. L., Van Hoeck, V., Gagne, D., Fournier, E., Thakur, A., O'doherty, A. M., Walsh, C. P., Sirard, M. A., Bols, P. E. & Leroy, J. L. 2016. Exposure of bovine oocytes and embryos to elevated non-esterified fatty acid concentrations: integration of epigenetic and transcriptomic signatures in resultant blastocysts. *BMC Genomics,* 17**,** 1004.

Desmet, K. L. J., Marei, W. F. A., Pintelon, I., Bols, P. E. J. & Leroy, J. 2018. The effect of elevated non-esterified fatty acid concentrations on bovine spermatozoa and on oocyte in vitro fertilisation. *Reprod Fertil Dev,* 30**,** 1553-1565.

Diez-Juan, A., Rubio, C., Marin, C., Martinez, S., Al-Asmar, N., Riboldi, M., Diaz-Gimeno, P., Valbuena, D. & Simon, C. 2015. Mitochondrial DNA content as a viability score in human euploid embryos: less is better. *Fertil Steril,* 104**,** 534-41 e1.

Dobbs, K. B., Rodriguez, M., Sudano, M. J., Ortega, M. S. & Hansen, P. J. 2013. Dynamics of DNA methylation during early development of the preimplantation bovine embryo. *PLoS One,* 8**,** e66230.

Duran, H. E., Simsek-Duran, F., Oehninger, S. C., Jones, H. W., Jr. & Castora, F. J. 2011. The association of reproductive senescence with mitochondrial quantity, function, and DNA integrity in human oocytes at different stages of maturation. *Fertil Steril,* 96**,** 384-8.

Funato, H., Oda, S., Yokofujita, J., Igarashi, H. & Kuroda, M. 2011. Fasting and high-fat diet alter histone deacetylase expression in the medial hypothalamus. *PLoS One,* 6**,** e18950.

Ge, Z. J. & Sun, Q.-Y. 2019. Maternal epigenetic inheritance. *In:* TOLLEFSBOL, T. O. (ed.) *Transgenerational Epigenetics (Second Edition).* Academic Press.

Ge, Z. J., Luo, S. M., Lin, F., Liang, Q. X., Huang, L., Wei, Y. C., Hou, Y., Han, Z. M., Schatten, H. & Sun, Q. Y. 2014. DNA methylation in oocytes and liver of female mice and their offspring: effects of high-fat-diet-induced obesity. *Environ Health Perspect,* 122**,** 159-64.

453 Gendelman, M. & Roth, Z. 2012. Incorporation of coenzyme Q10 into bovine oocytes improves mitochondrial
454 features and alleviates the effects of summer thermal stress on developmental competence. *Biol Reprod,*
455 87**,** 118.
456 Grindler, N. M. & Moley, K. H. 2013. Maternal obesity, infertility and mitochondrial dysfunction: potential
457 mechanisms emerging from mouse model systems. *Mol Hum Reprod,* 19**,** 486-94.
458 Gu, L., Wang, Q. & Sun, Q. Y. 2010. Histone modifications during mammalian oocyte maturation: dynamics,
459 regulation and functions. *Cell Cycle,* 9**,** 1942-50.
460 Guenther, M. G., Yu, J. J., Kao, G. D., Yen, T. J. & Lazar, M. A. 2002. Assembly of the SMRT-histone
461 deacetylase 3 repression complex requires the TCP-1 ring complex. *Genes & Development,* 16**,** 3130-
462 3135.
463 Hackett, J. A. & Surani, M. A. 2013. DNA methylation dynamics during the mammalian life cycle. *Philos Trans*
464 *R Soc Lond B Biol Sci,* 368**,** 20110328.
465 Harvey, A. J. 2019. Mitochondria in early development: linking the microenvironment, metabolism and the
466 epigenome. *Reproduction,* 157**,** R159-R179.
467 Hou, Y.-J., Zhu, C.-C., Duan, X., Liu, H.-L., Wang, Q. & Sun, S.-C. 2016. Both diet and gene mutation induced
468 obesity affect oocyte quality in mice. *Scientific Reports,* 6**,** 18858.
469 Igosheva, N., Abramov, A. Y., Poston, L., Eckert, J. J., Fleming, T. P., Duchen, M. R. & Mcconnell, J. 2010.
470 Maternal diet-induced obesity alters mitochondrial activity and redox status in mouse oocytes and
471 zygotes. *PLoS One,* 5**,** e10074.
472 Ispada, J., Da Fonseca Junior, A. M., Santos, O. L. R., Bruna De Lima, C., Dos Santos, E. C., Da Silva, V. L.,
473 Almeida, F. N., De Castro Leite, S., Juan Ross, P. & Milazzotto, M. P. 2021. Metabolism-driven post-
474 translational modifications of H3K9 in early bovine embryos. *Reproduction,* 162**,** 181-191.
475 Kim, J.-M., Liu, H., Tazaki, M., Nagata, M. & Aoki, F. 2003. Changes in histone acetylation during mouse
476 oocyte meiosis. *The Journal of cell biology,* 162**,** 37-46.
477 Krisher, R. L. & Prather, R. S. 2012. A role for the Warburg effect in preimplantation embryo development:
478 metabolic modification to support rapid cell proliferation. *Mol Reprod Dev,* 79**,** 311-20.
479 Lee, O. & O'brien, P. J. 2010. 1.19 - Modifications of Mitochondrial Function by Toxicants. *In:* MCQUEEN, C.
480 A. (ed.) *Comprehensive Toxicology (Second Edition).* Oxford: Elsevier.
481 Leist, M., Single, B., Castoldi, A. F., Kühnle, S. & Nicotera, P. 1997. Intracellular adenosine triphosphate (ATP)
482 concentration: a switch in the decision between apoptosis and necrosis. *J Exp Med,* 185**,** 1481-6.

Li, X. Y., Qin, Y. J., Wang, Y., Huang, T., Zhao, Y. H., Wang, X. H., Martyniuk, C. J. & Yan, B. 2021. Relative comparison of strobilurin fungicides at environmental levels: Focus on mitochondrial function and larval activity in early staged zebrafish (Danio rerio). *Toxicology,* 452**,** 152706.

Lu, C. & Thompson, C. B. 2012. Metabolic regulation of epigenetics. *Cell Metab,* 16**,** 9-17.

Marei, W. F. A., Ghafari, F. & Fouladi-Nashta, A. A. 2012. Role of hyaluronic acid in maturation and further early embryo development of bovine oocytes. *Reproduction in Domestic Animals,* 47**,** 454-454.

Marei, W. F. A., Van Den Bosch, L., Pintelon, I., Mohey-Elsaeed, O., Bols, P. E. J. & Leroy, J. 2019. Mitochondria-targeted therapy rescues development and quality of embryos derived from oocytes matured under oxidative stress conditions: a bovine in vitro model. *Hum Reprod,* 34**,** 1984-1998.

Marei, W. F. A., Smits, A., Mohey-Elsaeed, O., Pintelon, I., Ginneberge, D., Bols, P. E. J., Moerloose, K. & Leroy, J. 2020. Differential effects of high fat diet-induced obesity on oocyte mitochondrial functions in inbred and outbred mice. *Sci Rep,* 10**,** 9806.

Matilainen, O., Quiros, P. M. & Auwerx, J. 2017. Mitochondria and Epigenetics - Crosstalk in Homeostasis and Stress. *Trends Cell Biol,* 27**,** 453-463.

Morgan, H. D., Santos, F., Green, K., Dean, W. & Reik, W. 2005. Epigenetic reprogramming in mammals. *Hum Mol Genet,* 14 Spec No 1**,** R47-58.

Mozzetta, C., Boyarchuk, E., Pontis, J. & Ait-Si-Ali, S. 2015. Sound of silence: the properties and functions of repressive Lys methyltransferases. *Nat Rev Mol Cell Biol,* 16**,** 499-513.

Muller, B., Lewis, N., Adeniyi, T., Leese, H. J., Brison, D. R. & Sturmey, R. G. 2019. Application of extracellular flux analysis for determining mitochondrial function in mammalian oocytes and early embryos. *Sci Rep,* 9**,** 16778.

Nagano, M., Katagiri, S. & Takahashi, Y. 2006a. ATP content and maturational/developmental ability of bovine oocytes with various cytoplasmic morphologies. *Zygote,* 14**,** 299-304.

Nagano, M., Katagiri, S. & Takahashi, Y. 2006b. Relationship between bovine oocyte morphology and in vitro developmental potential. *Zygote,* 14**,** 53-61.

O'doherty, A. M., O'shea, L. C. & Fair, T. 2012. Bovine DNA methylation imprints are established in an oocyte size-specific manner, which are coordinated with the expression of the DNMT3 family proteins. *Biol Reprod,* 86**,** 67.

O'doherty, A. M., O'gorman, A., Al Naib, A., Brennan, L., Daly, E., Duffy, P. & Fair, T. 2014. Negative energy balance affects imprint stability in oocytes recovered from postpartum dairy cows. *Genomics,* 104**,** 177-185.

Okano, M., Bell, D. W., Haber, D. A. & Li, E. 1999. DNA methyltransferases Dnmt3a and Dnmt3b are essential for de novo methylation and mammalian development. *Cell,* 99**,** 247-257.

Paczkowski, M., Silva, E., Schoolcraft, W. B. & Krisher, R. L. 2013. Comparative importance of fatty acid beta-oxidation to nuclear maturation, gene expression, and glucose metabolism in mouse, bovine, and porcine cumulus oocyte complexes. *Biol Reprod,* 88**,** 111.

Pfaffl, M. W. 2001. A new mathematical model for relative quantification in real-time RT-PCR. *Nucleic Acids Res,* 29**,** e45.

Piersanti, R. L., Horlock, A. D., Block, J., Santos, J. E. P., Sheldon, I. M. & Bromfield, J. J. 2019. Persistent effects on bovine granulosa cell transcriptome after resolution of uterine disease. *Reproduction,* 158**,** 35-46.

Ross, P. J. & Sampaio, R. V. 2018. Epigenetic remodeling in preimplantation embryos: cows are not big mice. *Anim Reprod,* 15**,** 204-214.

Sakatani, M., Bonilla, L., Dobbs, K. B., Block, J., Ozawa, M., Shanker, S., Yao, J. & Hansen, P. J. 2013. Changes in the transcriptome of morula-stage bovine embryos caused by heat shock: relationship to developmental acquisition of thermotolerance. *Reprod Biol Endocrinol,* 11**,** 3.

Schierding, W., Vickers, M. H., O'sullivan, J. M. & Cutfield, W. S. 2017. 9 - Epigenetics. *In:* POLIN, R. A., ABMAN, S. H., ROWITCH, D. H., BENITZ, W. E. & FOX, W. W. (eds.) *Fetal and Neonatal Physiology (Fifth Edition).* Elsevier.

Smiraglia, D. J., Kulawiec, M., Bistulfi, G. L., Gupta, S. G. & Singh, K. K. 2008. A novel role for mitochondria in regulating epigenetic modification in the nucleus. *Cancer biology & therapy,* 7**,** 1182-1190.

Smith, Z. D., Chan, M. M., Mikkelsen, T. S., Gu, H., Gnirke, A., Regev, A. & Meissner, A. 2012. A unique regulatory phase of DNA methylation in the early mammalian embryo. *Nature,* 484**,** 339-44.

Stojkovic, M., Machado, S. A., Stojkovic, P., Zakhartchenko, V., Hutzler, P., Goncalves, P. B. & Wolf, E. 2001. Mitochondrial distribution and adenosine triphosphate content of bovine oocytes before and after in vitro maturation: correlation with morphological criteria and developmental capacity after in vitro fertilization and culture. *Biol Reprod,* 64**,** 904-9.

Sturmey, R. G., Reis, A., Leese, H. J. & Mcevoy, T. G. 2009. Role of fatty acids in energy provision during oocyte maturation and early embryo development. *Reprod Domest Anim,* 44 Suppl 3**,** 50-8.

Sukur, G., Uysal, F. & Cinar, O. 2023. High-fat diet induced obesity alters Dnmt1 and Dnmt3a levels and global DNA methylation in mouse ovary and testis. *Histochem Cell Biol,* 159**,** 339-352.

Symersky, J., Osowski, D., Walters, D. E. & Mueller, D. M. 2012. Oligomycin frames a common drug-binding site in the ATP synthase. *Proc Natl Acad Sci U S A,* 109**,** 13961-5.

Temple, I. K. & Shield, J. P. 2002. Transient neonatal diabetes, a disorder of imprinting. *J Med Genet,* 39**,** 872-5.

Teperino, R., Schoonjans, K. & Auwerx, J. 2010. Histone Methyl Transferases and Demethylases; Can They Link Metabolism and Transcription? *Cell Metabolism,* 12**,** 321-327.

Uh, K., Ryu, J., Farrell, K., Wax, N. & Lee, K. 2020. TET family regulates the embryonic pluripotency of porcine preimplantation embryos by maintaining the DNA methylation level of NANOG. *Epigenetics,* 15**,** 1228-1242.

Valckx, S. D. M., De Pauw, I., De Neubourg, D., Inion, I., Berth, M., Fransen, E., Bols, P. E. J. & Leroy, J. L. M. R. 2012. BMI-related metabolic composition of the follicular fluid of women undergoing assisted reproductive treatment and the consequences for oocyte and embryo quality. *Human Reproduction,* 27**,** 3531-3539.

Van Der Reest, J., Nardini Cecchino, G., Haigis, M. C. & Kordowitzki, P. 2021. Mitochondria: Their relevance during oocyte ageing. *Ageing Res Rev,* 70**,** 101378.

Wang, Q., Ratchford, A. M., Chi, M. M., Schoeller, E., Frolova, A., Schedl, T. & Moley, K. H. 2009. Maternal diabetes causes mitochondrial dysfunction and meiotic defects in murine oocytes. *Mol Endocrinol,* 23**,** 1603-12.

Wellen, K. E., Hatzivassiliou, G., Sachdeva, U. M., Bui, T. V., Cross, J. R. & Thompson, C. B. 2009. ATP-citrate lyase links cellular metabolism to histone acetylation. *Science,* 324**,** 1076-80.

Wu, X., Hu, S., Wang, L., Li, Y. & Yu, H. 2020. Dynamic changes of histone acetylation and methylation in bovine oocytes, zygotes, and preimplantation embryos. *J Exp Zool B Mol Dev Evol,* 334**,** 245-256.

Wydooghe, E., Vandaele, L., Beek, J., Favoreel, H., Heindryckx, B., De Sutter, P. & Van Soom, A. 2011. Differential apoptotic staining of mammalian blastocysts based on double immunofluorescent CDX2 and active caspase-3 staining. *Anal Biochem,* 416**,** 228-30.

Yin, X. & Xu, Y. 2016. Structure and Function of TET Enzymes.

Figures

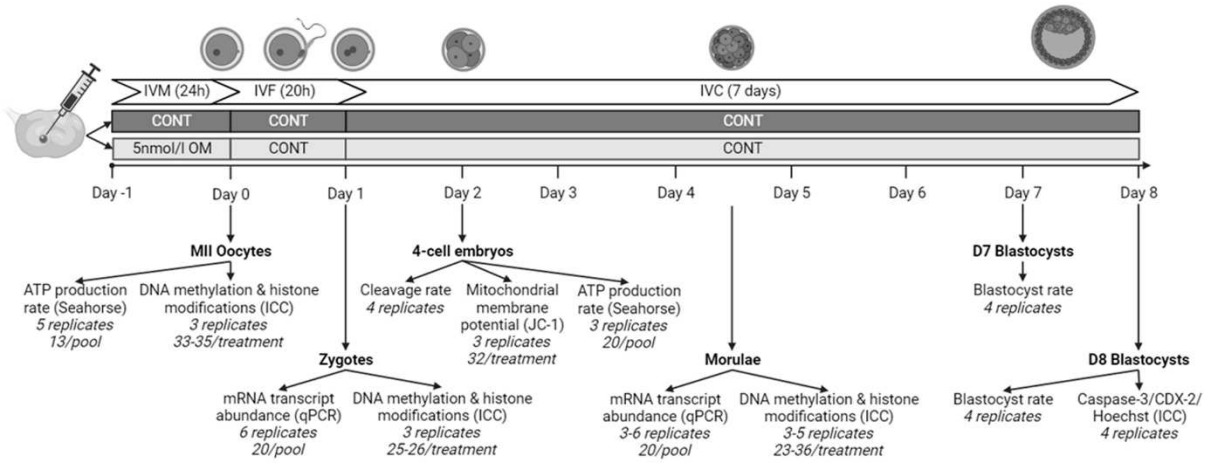

Fig. 1: Overview of the experimental design. Bovine cumulus-oocyte complexes were exposed to control (CONT) or 5nmol/l oligomycin A (OM) during *in* vitro maturation (IVM). IVF = *in vitro* fertilisation, IVC = *in vitro* culture, ICC = immunocytochemistry, qPCR = quantitative polymerase chain reaction, JC-1 = (5,5',6,6'-tetrachloro-1,1',3,3'-tetraethyl-benzimidazolyl-carbocyanine iodide), MMP = mitochondrial membrane potential. Created with BioRender.com.

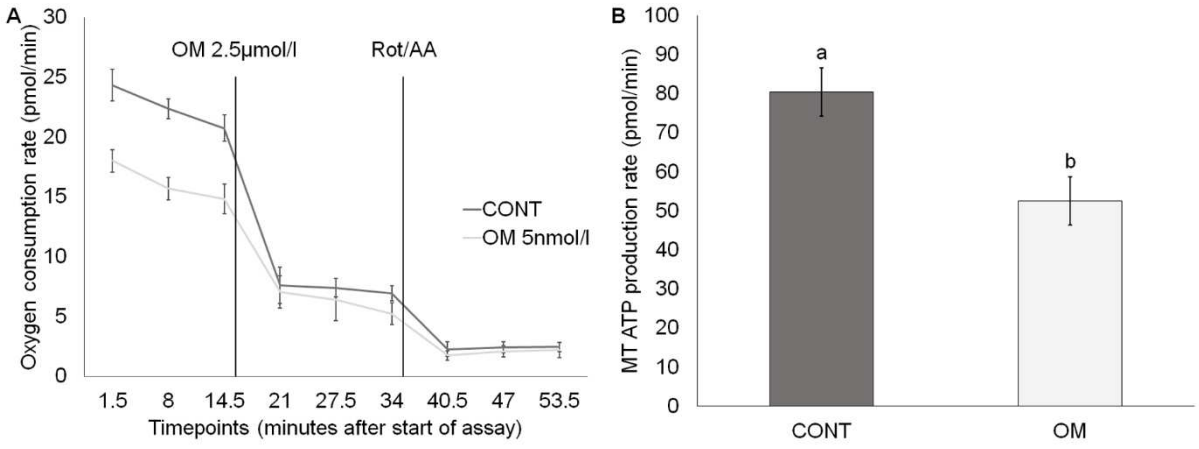

Fig. 2: (a) Kinetic graph of the average bovine MII oocyte oxygen consumption rate (OCR) of all replicates for the oligomycin (OM) and control (CONT) group. (b) Mitochondrial ATP production rate in bovine MII oocytes from the CONT and OM group. Each bar shows mean +/- SEM. Significant differences ($P \leq 0.05$) are shown by different letters (a or b).

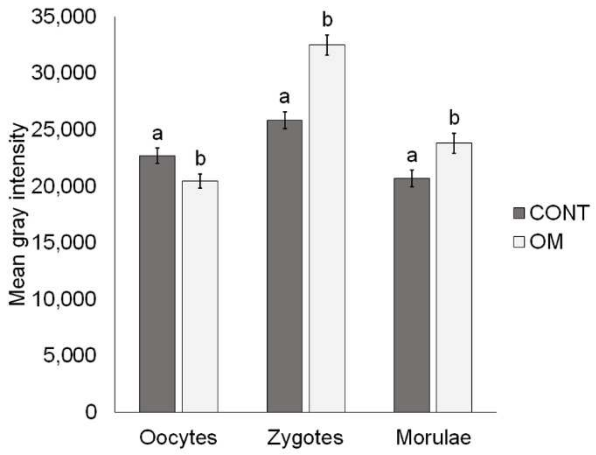

582

583 **Fig. 3**: 5mC levels in bovine oocytes, zygotes, and morulae from the control (CONT) group and oligomycin (OM)

584 group. Each bar shows mean +/- SEM. Significant differences ($P \leq 0.05$) are shown by different letters (a or b).

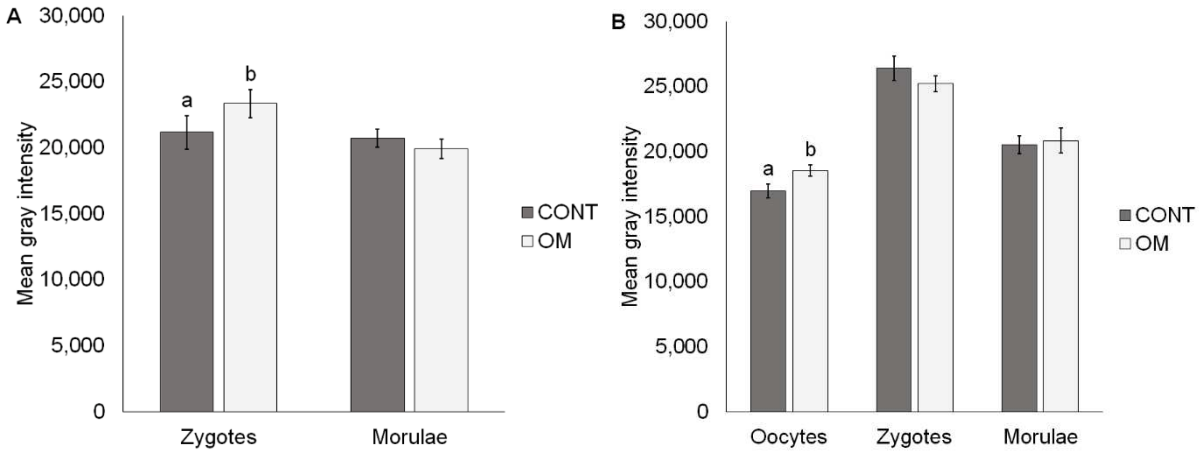

585

586 **Fig. 4**: (a) H3K9ac levels in bovine zygotes, and morulae from the control (CONT) group and oligomycin (OM)

587 group. (b) H3K9me2 levels in bovine oocytes, zygotes, and morulae from the CONT group and OM group. Each

588 bar shows mean +/- SEM. Significant differences ($P \leq 0.05$) are shown by different letters (a or b).

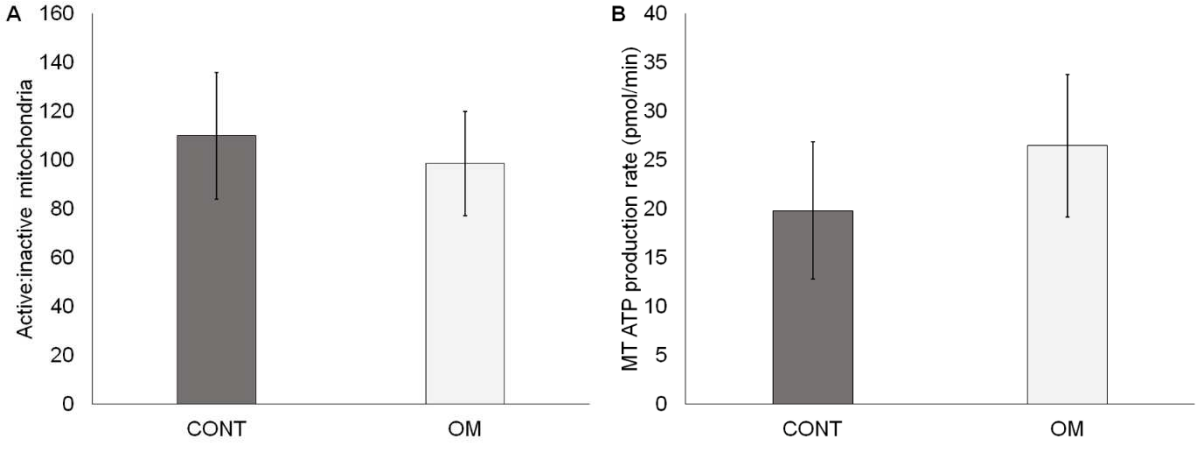

589

Fig. 5: (a) Quantification of mitochondrial membrane potential (MMP) by calculating the ratio of j-aggregates (active mitochondria) to monomers (inactive mitochondria) using JC-1 staining in bovine 4-cell embryos. (b) Measurement of mitochondrial ATP production rate using the Seahorse XF Mini Bioanalyzer in bovine 4-cell embryos derived from control (CONT) oocytes and oligomycin (OM)-exposed oocytes. Data are presented as mean +/- SEM.

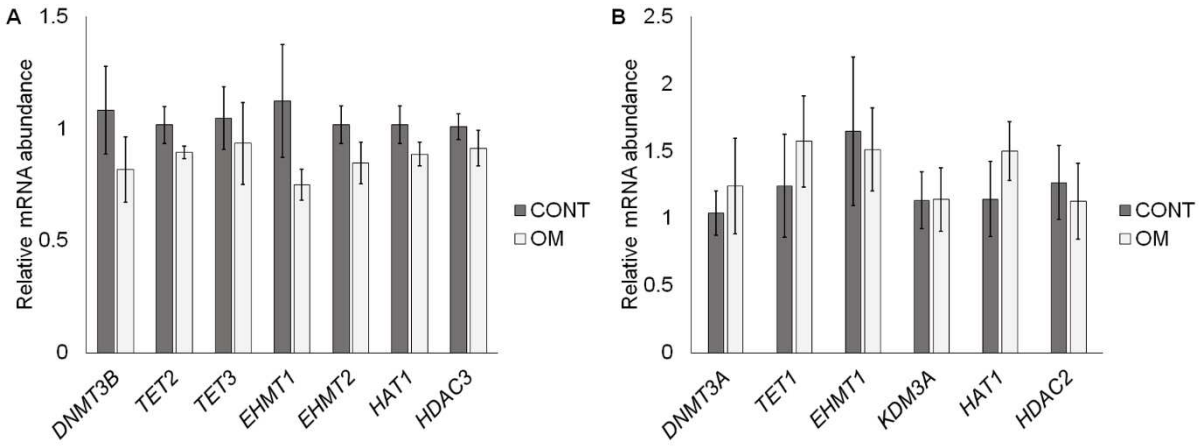

Fig. 6: Expression of epigenetic regulatory genes in bovine (a) zygotes and (b) morulae derived from control (CONT) and oligomycin (OM)-treated cumulus-oocyte complexes. Data are presented as mean +/- SEM.

Tables

Table 1: Epigenetic regulatory genes that were used for qPCR in bovine zygotes and morulae.

	Zygote	**Morula**
DNA methylation	*DNMT3B*	*DNMT3A*
DNA demethylation	*TET2, TET3*	*TET1*
Histone methylation	*EHMT1, EHMT2*	*EHMT1*
Histone demethylation	-	*KDM3A*
Histone acetylation	*HAT1*	*HAT1*
Histone deacetylation	*HDAC3*	*HDAC2*

Primers were designed using the Primer-BLAST tool, are exon spanning, and based on Reference sequences of *Bos taurus* from the National Center for Biotechnology Information (NCBI). See Supplementary Table 2 for full primer list.

DNMT3A/B, DNA methyltransferase 3 alpha/beta; *TET1/2/3*, ten-eleven translocase methylcytosine dioxygenase 1/2/3; *EHMT1/2*, euchromatic histone-lysine *N*-methyltransferase 1/2; *KDM3A*, lysine demethylase 3a; *HAT1*, histone acetyltransferase 1; *HDAC2/3*, histone deacetylase 2/3.

605 **Table 2**: Effect of OM-exposure on bovine embryo cleavage rates and day 7 & day 8 blastocyst rates (n = 4).

	CONT	**OM**	***P*-value**
Total COCs (n)	387	381	/
Cleaved embryos (%)	319 (82.4) [a]	290 (76.1) [b]	0.031
4-cell stage or more (%)	212 (54.8) [a]	189 (49.6) [a]	0.151
Fragmented embryos (%)	67 (17.3) [a]	56 (14.7) [a]	0.324
Day 7 blastocysts (% from total COCs)	98 (25.3) [a]	83 (21.8) [a]	0.248
Day 8 blastocysts (% from total COCs)	134 (34.6) [a]	107 (28.1) [a]	0.051
Day 8 blastocysts (% from cleaved embryos)	134 (42.0) [a]	107 (36.9) [a]	0.198

606 Data are shown as total numbers (and proportions within parentheses, %). Different letters (a or b) represent statistical
607 significance ($P \leq 0.05$). COC, cumulus–oocyte complex; CONT, control; OM, oligomycin.

608 **Table 3**: The effect of OM-exposure on day 8 bovine blastocyst quality.

	CONT	**OM**	***P*-value**
All blastocysts			
Total blastocysts (n)	103	74	/
Total cell count (n)	133.7 ± 4.5 [a]	121.1 ± 5.0 [a]	0.071
Apoptotic cell index (%)	7.3 ± 0.5 [a]	10.3 ± 0.7 [b]	<0.001
Early blastocysts only			
Total blastocysts (n)	17	10	/
Total cell count (n)	87.5 ± 5.8 [a]	76.6 ± 7.1 [a]	0.264
TE cell count (n)	57.6 ± 4.4 [a]	50.2 ± 7.3 [a]	0.721
ICM cell count (n)	29.9 ± 2.1 [a]	26.4 ± 2.0 [a]	0.442
TE/ICM ratio (n)	2.0 ± 0.1 [a]	2.0 ± 0.3 [a]	0.959
Apoptotic cell index (%)	10.6 ± 2.0 [a]	10.1 ± 3.4 [a]	0.551
Advanced blastocysts only			

Total blastocysts (n)	86	64	/
Total cell count (n)	145.4 ± 4.2 [a]	131.6 ± 4.6 [b]	0.018
TE cell count (n)	99.7 ± 3.1 [a]	88.4 ± 3.3 [b]	0.009
ICM cell count (n)	45.4 ± 1.3 [a]	44.1 ± 1.7 [a]	0.458
TE/ICM ratio (n)	2.2 ± 0.1 [a]	2.1 ± 0.1 [a]	0.083
Apoptotic cell index (%)	6.9 ± 0.5 [a]	10.0 ± 0.7 [b]	<0.001

Different letters (a or b) represent statistical significance ($P \leq 0.05$). Total cell count = total number of cells that were counted for each blastocyst, i.e. the sum of the amount of trophectoderm cells and inner cell mass cells. Apoptotic cell index was calculated as the total number of apoptotic cells on the total cell count. Early blastocysts = young and normal; advanced blastocysts = expanded and hatched. Data are shown as means ± S.E.M. CONT, control; ICM, inner cell mass; OM, oligomycin; TE, trophectoderm.